

# Numerical Simulation on Two-Dimensional Detonation including Boundary Layer Effects

Nobuyuki Tsuboi<sup>1</sup>, Youhi Morii<sup>2</sup>, A.Koichi Hayashi<sup>3</sup>, Mitsuo Koshi<sup>4</sup>

<sup>1</sup>Department of Mechanical and Control Engineering, Kyushu Institute of Technology,  
1-1 Sensui-cho, Tobata-ku, Kitakyusyu, Fukuoka 804-8550, Japan

<sup>2</sup>Department of Space and Astronautical Science, The Graduate University of Advanced Studies,  
3-1-1 Yoshinodai, Chuo-ku, Sagamihara, Kanagawa 252-5210, Japan

<sup>3</sup>Department of Mechanical Engineering, Aoyama Gakuin University,  
5-10-1 Fuchinobe, Chuo-ku, Sagamihara, Kanagawa 252-5285, Japan

<sup>4</sup>Faculty of Engineering, The University of Tokyo,  
2-11-16 Yayoi, Bunkyo-ku, Tokyo 113-8656, Japan

## 1 Introduction

Detonation is a shock-induced combustion wave propagating through a reactive mixture or pure exothermic compound, and has been studied from the safety engineering point of view such as for coal mine explosions or from the scientific point of view of astrophysics as in star explosions. Numerical simulations on the detonations usually neglect viscous and thermal loss terms in the governing equations because its propagation speed is supersonic and the pressure at Chapman-Jouget state is approximately 20 times the initial pressure. However, the propagations near the detonation limit are affected by the viscous and thermal losses and the detonation becomes a single-spinning mode. Campbell and Woodhead first discovered a spinning detonation in a stoichiometric mixture of carbon monoxide and oxygen in 1926 [1, 2, 3]. Bone and co-workers systematically investigated the detonation phenomena to conclude that spin was connected with the mode of coupling between the leading shock front and the reaction zone [4, 5, 6]. The spinning detonation is found to propagate stably in the tube [7, 8]. The detonation velocity of the spinning detonation is approximately 80~90% of  $D_{CJ}$  and this reason is thought to be the viscous and thermal loss effects [7]. Haloua et al. [9] identified four modes of propagation for the detonations in a tube by varying the initial pressure of a given mixture of  $C_2H_2/O_2$  or by changing the dilution. Those four modes are stable detonation, stuttering mode, galloping mode, and fast flame. The stuttering behavior can be associated with the spinning detonations [10].

These detonation velocity deficits can be evaluated by means of the ZND (Zel'dovich-Neumann-Doring) simulations including the viscous and thermal losses [7, 11]. One parameter in these simulations, which changes the amount of friction and heat losses, control the effects of their losses as the numerical results agree with the experimental results. Fay [12] found that the magnitude of the velocity deficit was consistent with the existence of the boundary layer by using an analytical method. However,

the release energy near the spin head also decreases near the detonation limit with decreasing the initial pressure. This means that the rotating transverse detonation in the spin head also becomes weak to decrease the propagating velocity. The dependency of the initial pressure on the release energy is also included in the CJ state, however, the multi-dimensional effects are not included. Therefore the effects of the release energy cannot be cleared on the two-dimensional and three-dimensional detonations. Furthermore, it should be evaluated whether the viscous and thermal losses or the reduction of the release energy dominate on the detonation velocity deficit under the low pressure conditions.

The aim of this work is to estimate the effects of the viscous loss and the boundary layer on the two-dimensional full Navier-Stokes simulations for hydrogen/air detonation under low pressure conditions. These results are also compared with the theoretical analysis in order to understand the mechanism of the velocity deficits near the limit of detonation.

## 2 Numerical Method

The governing equations are the full Navier-Stokes(NS) equations with 9 species ( $H_2$ ,  $O_2$ , H, O, OH,  $HO_2$ ,  $H_2O_2$ ,  $H_2O$ , and  $N_2$ ) and 18 elementary reactions, and are explicitly integrated by the Strang type fractional step method. The chemical reaction source terms are treated in a linearly point-implicit manner in order to avoid a stiff problem. A second-order Harten-Yee non-MUSCL type TVD scheme is used for the numerical flux in the convective terms[13]. The second-order central differential is used for the viscous term. Turbulent models are not included in these simulations. The present code can predict the laminar boundary layer profiles behind the moving shock wave as shown in Ref. [14]. The Petersen and Hanson model[15] is used for chemical kinetics to solve detonation problems. This model contains 18 reactions and 9 species, and it is based on the  $H_2/O_2$  submechanism of the RAMEC/Gas Research Institute GRI-Mech 1.2 methane-oxidation mechanism.

The computational meshes are shown in Fig. 2. The present grids consist of three grids. The summary of the present grid system is shown in Table.1. Zone 1 is used near the detonation front and its propagating resolution,  $\Delta x$ , is  $25 \mu m$ . Zone 3 is for the reward domain with  $100 \mu m$  or coarser resolution. Zone 2 connects between zone 1 and zone 3. All grids have minimum grid width of 25 or  $10 \mu m$  near the walls. The grid points of zone 1, 2, and 3 in grid 1 are  $801 \times 301$ ,  $201 \times 151$ , and  $401 \times 76$  and those in grid 2 are  $4001 \times 401$ ,  $201 \times 201$ , and  $401 \times 101$  for  $d=7.5$  mm, respectively. As the channel width increases, the number of grid points normal to the propagating direction also increases. 25 and  $10 \mu m$  corresponds to a resolution of 64 and 160 grid points in the theoretical half reaction length which equals  $1.6 \times 10^{-3} m$  for  $H_2$  at  $p_0 = 0.1$  atm. Then channel width,  $d$ , varies from 5 mm to 20 mm. The scales of the computational domain are also shown in Table.1.

The boundary conditions are as follows: the upstream conditions are a pressure of 0.1 atm and a temperature of 300 K, and the upstream gas is a stoichiometric  $H_2/air$ ; the wall boundary conditions are adiabatic, non-slip, and non-catalytic; and the downstream condition is that a non-reflection boundary proposed by Gamezo et al.[16] is imposed. Therefore the present simulations only estimate the viscous effects because the thermal loss cannot be calculated in the adiabatic wall condition. Reynolds number based on the channel width, which defines as  $Re_d = \rho_{CJ} a_{CJ} d / \mu_{CJ}$ , is approximately  $2.64 \times 10^4$  for  $d = 10$  mm.  $Re_d$  is the order of  $10^4$  therefore the laminar assumption is possible to discuss about the present simulations. A transition from the laminar boundary layer to turbulent one would appear at far downstream from the detonation front, therefore the turbulent effects should be included in the future work. The present simulations adopt the moving grid system instead of the wave coordinate system because a carbuncle at the detonation front, which is one of the numerical instability near shock front, appears near the wall in the wave coordinate system. The wave coordinate system for non-slip boundary

sets velocity as CJ value along the wall, and this causes peak velocities along the direction normal to the wall. The moving grid system means that the computational grid moves with a specified velocity and the velocity along the wall set to zero. In the present simulations, the computational grid move with 80% of CJ velocity. The time-dependent metrics are included in the present numerical schemes.

Table 1: Scale of computational domain and resolution.

	$d$ (mm)	$L$ (mm)	$L_1$ (mm)	$\Delta y_{min}$ ( $\mu m$ )
Grid 1	5 ~ 20	249	20	25
Grid 2 (fine grid)	5 ~ 20	329	100	10

### 3 Results and Discussions

The present simulations use coarse grid(grid 1) and fine grid(grid 2) near the wall. The minimum grid sizes near the wall,  $\Delta y_{min}$ , are 25  $\mu m$  and 10  $\mu m$ , respectively. The following discussion is based on the results using grid 2.

#### 3.1 Boundary-layer resolution over flat plate

Two cases are simulated to evaluate the laminar boundary layer resolutions on the present code. First test is to simulate a laminar boundary layer development over a flat plate in air. Free stream Mach number, pressure, and temperature are 0.5, 0.01 atm, and 300 K, respectively. The length of the flat plate is 2 m and the height of the computational domain is 2 m. Reynolds number is  $1.2 \times 10^5/m$ . Minimum grid scale near the plate,  $\Delta y$ , is  $6.3 \times 10^{-5}$  m. The wall boundary sets adiabatic and nonslip. Figure 1 show that the present results agree well with the Blasius theoretical profiles. Therefore the present code is able to simulate laminar boundary layer.

Next test is to solve a shock induced laminar boundary layer over a flat plate in air. The shock Mach number is 1.9, Reynolds number is  $= 50 \times 10^6/m$ , initial pressure is 1 atm, and initial temperature is 300 K, respectively. The channel width is 3 mm and minimum grid size near the bottom wall is 0.5  $\mu m$ . The wall boundary is adiabatic and nonslip. The results and the comparison with the theories are shown in Fig.1. The velocity profiles in the boundary layer agree well with the shock induced laminar boundary layer theory proposed by Sturtevant et al[17]. The velocity gradient in the boundary layer behind the moving shock wave is 60% larger than the Blasius theory. Therefore the present code is able to simulate compressible boundary layer behind a moving shock wave.

#### 3.2 Channel width effects on velocity deficits

The channel width effects on the average detonation velocity are presented in Fig. 2. The calculated results by using the modified ZND with and without heat loss[7] are plotted in this figure. The parameter  $\eta$  to control viscosity changes between 0.25 and 1.0 in the modified ZND calculations. The grid resolution effects between grid 1 and grid 2 on average detonation velocities are also shown in this figure.

The detonation velocities in the inviscid simulations do not affected by the channel width and the detonation propagates with CJ velocity. The viscous simulations show that the detonation velocities are lower than the CJ velocity. As the channel width decreases, the velocity deficits increase for both grid systems. The grid resolution dependency between grid 1 and grid 2 is about 1% on the average detonation velocity. The velocity deficit on grid 2 is 3.4 % for  $d=10$  mm, 5% for  $d=7.5$  mm, and 8% for  $d=5$  mm, respectively. The velocity deficits increase rapidly as the channel width is smaller than 10 mm.

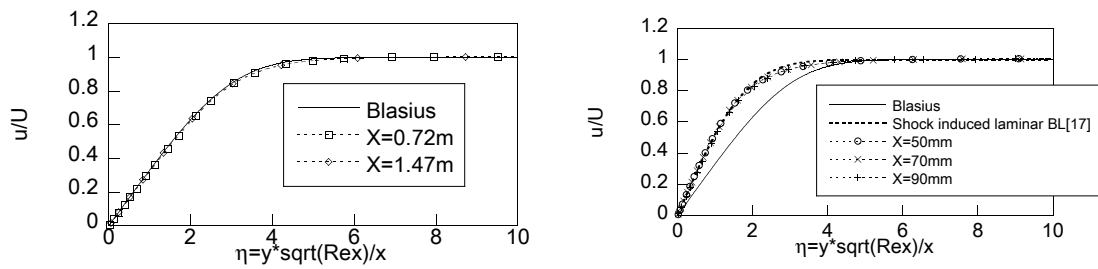


Figure 1: Velocity profiles over flat plate. Left: Laminar boundary layer. Right: Shock-induced boundary layer.

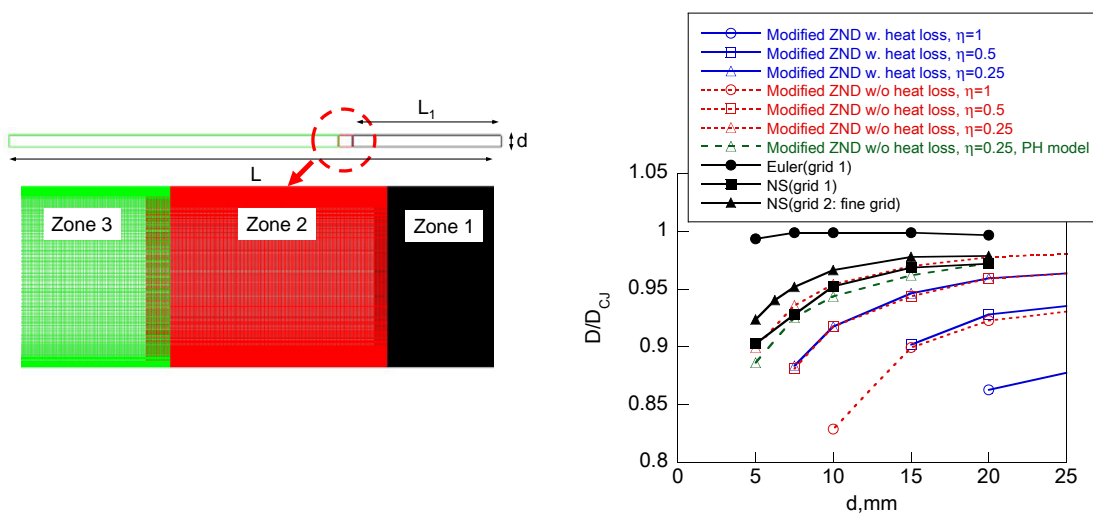


Figure 2: Computational grid system and detonation velocity. Left: Present grid system(grid 2). Right: Average detonation velocities.

The effects of heat loss on the modified ZND simulations show that the amount of heat loss is approximately equal to that of friction loss because the case with heat loss ( $\eta = 0.25$ ) agrees with the case without heat loss ( $\eta = 0.5$ ). Therefore the present discussions focus on the effects of friction loss under the detonation limit in order to find the influence of loss on the detonation. The comparison between Koshi model and Petersen and Hanson model (PH model) on the modified ZND simulations for  $\eta = 0.25$  shows that the difference between them is approximately 1% and their trends agree well due to low initial pressure. The friction loss  $\sigma$  in the present modified ZND theory is derived assuming the round tube, therefore  $\eta = 0.5$  is acceptable for two-dimensional channel due to the ratio of the core flow area to the boundary layer displacement area at cross section. The comparison between NS(grid 2) and modified ZND at  $d=10$  mm, NS(grid 2) is 2~3% higher than the modified ZND ( $\eta = 0.5$ , w/o heat loss), however, NS(grid 2) agree well with modified ZND ( $\eta = 0.25$ , w/o heat loss). The modification of  $\sigma$  on the modified ZND will be necessary for two-dimensional channel while overall trend agrees between NS and modified ZND. NS(grid 1) for lower than  $d < 5$  mm cannot be simulated due to a decoupling phenomena between the shock front and the detonation front. NS(grid 1) for  $d = 5$  mm becomes very unstable due to the similar decoupling phenomena.

### 3.3 Boundary layer effects behind detonation front

The present section discusses about the feature of the detonation near the detonation limit for  $d=7.5$  and 10 mm on grid 2.

As shown in Fig. 2, the velocity deficit is 3.4 % for  $d=10$  mm while the detonation stably propagates as shown in Fig. 3(b). In this channel width, the detonation cells are clearly observed and the cell length does not change. However, the detonation for  $d=7.5$  mm propagates with a periodical oscillation as shown in Fig. 3(a), in which the velocity deficit is 5%. Time histories of local specific energy release in Figs. 3(c),(d) also show similar feature and the heat release for  $d=7.5$  mm is lower than that for  $d=10$  mm. This means that the detonation weakens due to viscous effects. These results would be compared with those with inviscid simulations in the future.

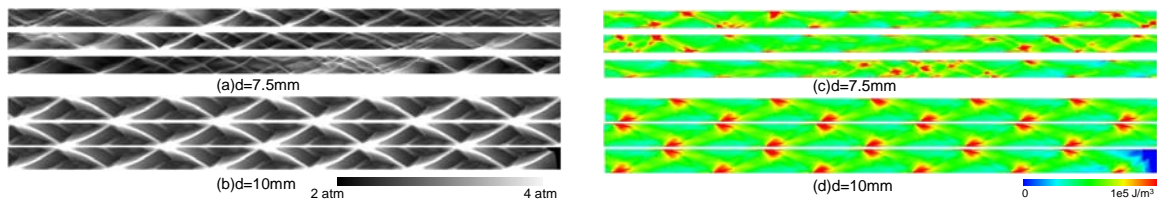


Figure 3: Effects of channel width(grid 2). Left: Maximum pressure history contours. Right: Time history of local specific energy release contours.

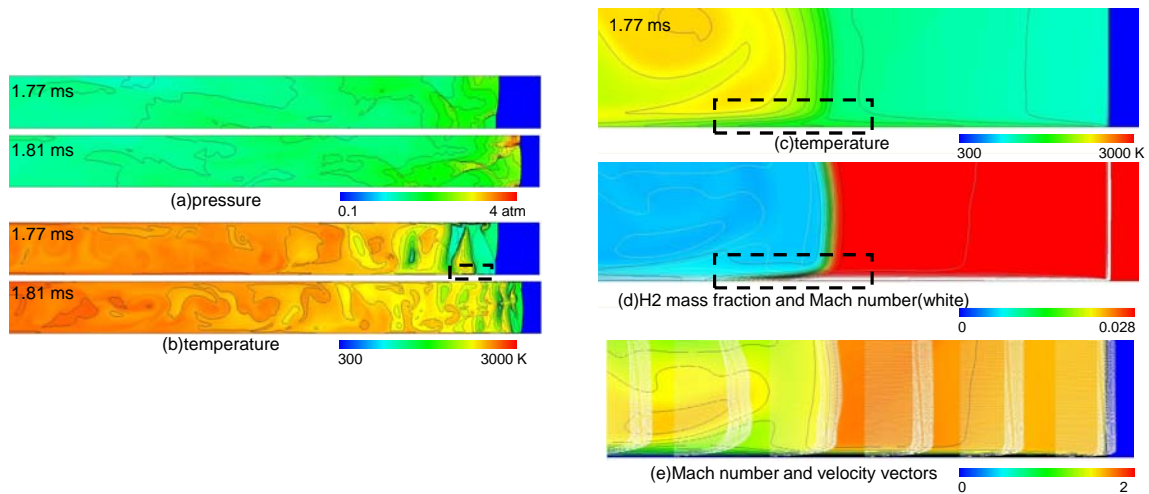


Figure 4: Instantaneous contours near detonation front for  $d=7.5$  mm(grid 2). Left: Pressure and temperature. Right: Close-up view of contours near wall.

For  $d=7.5$  mm, the detonation propagates with an periodical oscillation and the instantaneous contours are shown in Fig. 4. At  $t=1.77$  msec, the triple point becomes unclear and the induction zone between the shock front and combustion front increases. At  $t=1.81$  msec, in the induction zone, an ignition appears and the triple point is clearly observed again. Figure 4(c)-(e) shows that the close-up view of temperature, H<sub>2</sub> mass fraction, and Mach number contours in the region of the broken line in Fig. 4(b)( $t=1.77$  ms). Mach number contours include velocity vectors in this figure. Temperature and H<sub>2</sub> mass fraction contours in zone of broken line in Fig. 4(c)(d) show that the flame front cannot penetrate into the boundary layer. The wall boundary layer has a velocity shear layer which is a large velocity

## **Tsuboi, N., et al Numerical Simulation on Two-Dimensional Detonation Including Boundary Layer Effects**

gradient. This means that Karlovitz number, which defines as  $K = (\partial U_e / \partial y)(\delta / U_e)$ [18] where  $U_e$  and  $\delta$  are velocity out of boundary layer and boundary layer thickness, is equal to one. Under  $K = 1 \sim 2$ , flame is stretched to delay propagation or quench. Therefore the present flame shape is strongly stretched by the wall boundary layer.

## **4 Conclusions**

Two-dimensional full Navier-Stokes simulations with the detailed chemistry model were performed for H<sub>2</sub>/air detonations in a channel in order to estimate the viscous loss effects on the detonation under the low pressure environment. The present NS code is confirmed to resolve the boundary layer by comparing with the theoretical results. The velocity deficit on the NS simulations fairly agree well with that on the modified ZND calculations neglecting the heat loss with  $\eta = 0.25$ . The velocity deficit on fine grid is 3.4 % for  $d=10$  mm though it is 5% for  $d=7.5$  mm. The velocity deficits increase rapidly as the channel width is smaller than 10 mm. The grid resolution effects on the velocity deficits are approximately 1%. The detonation for  $d > 10$  mm stably propagates in the channel while that for  $d < 10$  mm becomes unstable. This feature coincides with the rapid increment of the velocity deficit for  $d < 10$  mm. As the channel width is lower than 10 mm, the leading shock and the flame front periodically separates and interacts, and the detonation becomes unstable. As the wall boundary layer has large velocity gradient, the flame front near the detonation front cannot propagate across the wall boundary layer. Karlovitz number near the wall is approximately one, therefore flame is stretched to delay propagation or quench. The present front flame shape near the wall is strongly stretched by the wall boundary layer.

## **Acknowledgments**

This research was collaborated with Cybermedia Center in Osaka University. This research was also supported by the Casio Science Promotion Foundation.

## **References**

- [1] C. Campbell, D.W. Woodhead, *J. Chem. Soc.* (1926) 3010-3021.
- [2] C. Campbell, D.W. Woodhead, *J. Chem. Soc.* (1927) 1572-1578.
- [3] C. Campbell, A.C. Finch, *J. Chem. Soc.* (1928) 2094-2106.
- [4] W.A. Bone, R.P. Fraser, *Phil. Trans. Roy. Soc.* A228, (1929) 197-234.
- [5] W.A. Bone, R.P. Fraser, *Phil. Trans. Roy. Soc.* A230, (1932) 363-385.
- [6] W.A. Bone, R.P. Fraser, Wheeler, W.H., *Phil. Trans. Roy. Soc.* A235, (1936) 29-68.
- [7] Kitano, S., Fukao, M., Susa, A., Tsuboi, N., Hayashi, A.K., Koshi, M., *Proc. Comb. Inst.* 32, (2009) 2355-2362.
- [8] Tsuboi, N., Hayashi, A. K., Koshi, M., *Proc. Comb. Inst.* 32, (2009) 2405-2412.
- [9] F. Haloua, M. Brouillette, V. Lienhart, G. Dupre, *Combust. Flame* 122, (2000) 422-438.
- [10] K. Ishii, H. Gronig, *Shock Waves* 8 (1998) 55-61.
- [11] Lee, J. H. S., *The Detonation Phenomenon*, Cambridge Univ. Press (2008).
- [12] J.A. Fay, *J. Chem. Phys.* 20, (1952) 942-950.
- [13] H.C. Yee, *NASA Technical Memorandum 89464* (1987).
- [14] N. Tsuboi, A.K. Hayashi, M. Koshi, 22nd International Colloquium on the Dynamics of Explosions and Reactive Systems, (2009) 145.
- [15] E.L. Petersen, R.K. Hanson, *J. Prop. Power* 15, (1999) 591-600 .
- [16] V.N. Gamezo, D. Desbordes, E.S. Oran, *Shock Waves* 9, (1999) 11-17.
- [17] B. Sturtevant, T.T. Okamura, *Physics of Fluids* 12, pp.1723-1725 (1969).
- [18] T. Niioka, M. Kono, J. Sato, *Principle of Combustion Phenomena*, Ohmsha, in Japanese (2001).